A flexoelectric microelectromechanical system on silicon

Umesh Kumar Bhaskar[1+], Nirupam Banerjee[2+], Amir Abdollahi[1], Zhe Wang[3], Darrell G. Schlom[3,4], Guus Rijnders[2], and Gustau Catalan[1,5]**

[1] *ICN2 – Institut Catala de Nanociencia i Nanotecnologia, CSIC and The Barcelona Institute of Science and Technology, Campus UAB, 08193 Bellaterra*

(Barcelona), Spain.

[2] *Faculty of Science and Technology and MESA+ Institute for Nanotechnology, University of Twente, P.O. Box 217, 7500 AE Enschede, The Netherlands*

[3] *Department of Materials Science and Engineering Cornell University, Ithaca, NY 14853, USA*

[4] *Kavli Institute at Cornell for Nanoscale Science, Ithaca, New York 14853, USA*

[5] *ICREA - Institucio Catalana de Recerca i Estudis Avançats, 08010 Barcelona, Spain*

KEYWORDS: flexoelectricity, MEMS, nanoscale, piezoelectrics

Flexoelectricity allows a dielectric material to polarize in response to a mechanical bending moment[1], and, conversely, to bend in response to an electric field[2]. Compared to piezoelectricity, flexoelectricity is a weak effect of little practical significance in bulk materials. However, the roles can be reversed at the nanoscale[3]. Here, we demonstrate that flexoelectricity is a viable

route to lead-free microelectromechanical and nanoelectromechanical systems (MEMS and NEMS). Specifically, we have fabricated a silicon compatible thin film cantilever actuator with a single flexoelectrically active layer of strontium titanate with a figure of merit (curvature divided by electric field) of 3.33 MV^{-1}, comparable to that of the state of the art piezoelectric bimorph cantilevers.

Main

Certain attributes of flexoelectricity point towards a favourable role in micro- and nano-electromechanical systems (MEMS and NEMS), for example: (i) Flexoelectricity is a universal phenomenon exhibited by materials of all symmetry groups, and thus flexoelectric devices can in principle be fabricated from silicon or any of its gate dielectrics in a completely complementary metal oxide semiconductor (CMOS) compatible environment; (ii) Any (strain) gradient scales inversely with the material dimension[3], thus allowing flexoelectricity to match or even dominate over piezoelectricity at the nanoscale[4], particularly in materials with high dielectric permittivity ε, such as ferroelectric thin film[5] and composites[6]; (iii) High frequency bending resonators capable of functioning at extreme temperatures can be implemented; (iv) Flexoelectric devices can be made from simple dielectrics, with a performance that is therefore linear and non-hysteretic, and (v) A flexoelectric, unlike a piezoelectric bimorph actuator, does not need to be clamped to an elastic passive layer in order to bend: a single dielectric layer is sufficient to achieve field-induced bending, and this simplifies device design and removes the risk of delamination that can exist in standard piezoelectric bimorph actuators (**Figure 1**).

In contrast, since the materials with the largest piezoelectric coefficients are ferroelectric, piezoelectric devices can suffer from their intrinsically hysteric nature and nonlinear behaviour at fields close to the coercive voltage, and in addition their properties are strongly temperature-dependent: they only work below their Curie temperature. Moreover, the ferroelectrics with largest piezoelectric coefficients are lead-based[7], and lead toxicity poses serious problems for integration of such devices in biomedical applications, where MEMS-based energy harvesting devices would otherwise find a natural niche of applications[8]. In addition, bimorphs can also be restricted by the mechanical and thermal expansion mismatch between the piezoelectric and elastic layer, which can lead to progressive deterioration of the bonding between layers.

Despite the advantages offered by nanoscale flexoelectricity, research in this field is still in its infancy[9,10], and considerable effort is required before it can be established as a viable technology. On the fundamental front, we need a reliable catalogue of flexoelectric coefficients for all materials of technological interest, and proof that the magnitude of these coefficients remains constant at the nanoscale. On the practical front, we need to develop both nanofabrication and nano-characterization tools suitable for making and measuring flexoelectric nanodevices. This article addresses both of these issues.

We fabricated all-oxide nanocantilevers **(Figure 2(a))** as capacitor structures consisting of a strontium titanate ($SrTiO_3$) active layer sandwiched between two layer of strontium ruthenate ($SrRuO_3$) for the top and bottom electrode; the complete capacitor stack (see Figure S1 and Figure S2) is epitaxially grown on a buffer of $SrTiO_3$ deposited by molecular beam epitaxy (MBE) on Si, which is currently an established template system for incorporating other epitaxial

oxide films on Si[11]. Fabrication details are provided in the methods section. The centrosymmetric lattice of room temperature $SrTiO_3$ ensures that any measured bending moment arises purely from flexoelecticity; room temperature paraelectricity in $SrTiO_3$ is also confirmed by its linear and non-hysteretic mechanical response as a function of electric field; for comparison, in the supplementary materials (See Figure S3) we show the characteristic butterfly-shape hysteresis loop response of a ferroelectric lead zirconium titanate (PZT) cantilever grown by similar methods on silicon. $SrTiO_3$ is also currently the only (bulk) material for which the theoretical and experimental values, measured using the direct method are of the same order of magnitude[12], providing a good reference for testing two important questions: (i) whether the bulk flexoelectric coefficients retain their bulk value in thin films and (ii) whether the coefficients measured by us via the inverse method (actuator mode) are the same as those measured in bulk by the direct method (sensor mode) –something that is definitely true for piezoelectrics but is not obvious in flexoelectricity, where this question has been controversial[13].

The most popular method currently used to characterize flexoelectric coefficients involves dynamically bending a cantilever and using lock-in techniques to instantaneously measure the charge generated by the bending. We refer to this as the direct method, and it has been employed on a variety of materials, including perovskite ceramics[14], single crystals[12], and even polymers[15]. Its drawback is the difficulty of miniaturizing mechanical bending appliances down to the nanoscale. But, while direct flexoelectricity measures the polarization induced by bending, a converse or inverse effect also exists whereby polarizing a sample causes it to bend[2,13,16,17,18]. The “inverse method” thus involves the application of an electric field to a cantilever or plate-shaped material, and measuring the induced bending[16,18]. The curvature (k) induced via

flexoelectricity (μ) is related to the flexural rigidity (D) of the plate and the applied voltage (V) by [9]:

$$k = \frac{\mu V}{D} \quad . \qquad (1)$$

The flexural rigidity (D) of a cantilever is $\frac{Et^3}{12(1-\nu^2)}$, where E is the young´s modulus, ν is the Poisson ratio, and t is the thickness. Hence, the flexoelectrically induced curvature k scales as the *cube* of the cantilever thickness, i.e., the voltage-induced bending multiplies by a factor of 8 –almost an order of magnitude- every time the thickness is halved. The inverse scaling of k with the Young´s modulus also makes it pertinent to characterizing soft materials, which are expected to display giant electromechanical couplings[19]. On the practical side, achieving converse flexoelectricity only requires the fabrication of planar capacitive cantilevers, and we demonstrate that this requirement can be readily realized using existing MEMS techniques. Thus, inverse flexoelectricity is an optimum route to exploring and exploiting the flexoelectricity of nanodevices.

The observation of cantilever oscillations induced by an applied alternate voltage (V_{ac}) was made using a commercial digital holographic microscope[20,21] (DHM) (schematically illustrated in **Figure 2(b) and 2(c)**) working in stroboscopic mode. The Fourier-filtered first harmonic displacement induced in the 16 x 40 um $SrTiO_3$ cantilever plate is plotted as a function of the AC excitation at 100 KHz and just above resonance (320 KHz) in **Figure 3(a)** and **3(b)** respectively (the unfiltered response at 100 KHz is shown in Figure S4). The curvature was calculated from the Fourier-filtered displacement[22]. In order to probe the dynamics further, the cantilever was excited with the same bias of 1 V but over a range of different sinusoidal frequencies (**Figure**

3(c)). The observed resonance frequency ~310 kHz corresponds quite well with the analytical estimation based on the geometry of the cantilever (see Figure S5), while the phase corresponds to the lag between the waveform of the excitation signal (voltage) and that of the flexoelectric response (deflection).

The first harmonic curvature measured as a function of applied AC field at ~100 KHz is plotted in **Figure 3(d)** and shows the expected linear behavior for a flexoelectric actuator. In order to demonstrate the stability of the measurements as a function of the frequency, we also include a complete curvature vs field measurement made at 10 KHz in figure S6. The value of the flexoelectric coefficient μ_{eff} calculated from the slope of curvature vs voltage using Equation 1 yields μ_{eff} ~ 4.6 nC/m. This is an effective flexoelectric coefficient involving a geometry-dependent combination of the flexoelectric tensor components. Calculations using a self-consistent continuum model of flexoelectricity[16] under the assumption that the ratio between μ_{11} and μ_{12} remains the same as in bulk[12] yield μ_{12} ~ 4.1 nC/m. This is comparable to the μ_{12} for bulk $SrTiO_3$ (100) crystals measured by the direct method (μ_{12} ~ 7 nC/m)[12], particularly when factoring in the smaller relative permittivity of our $SrTiO_3$ thin film, which is ~four times smaller compared to that of bulk single crystals. Indeed, the quantity of physical significance[9] is the flexocoupling ratio $f = \frac{\mu}{\varepsilon}$, which we found to be 6 V for $SrTiO_3$ nanocantilevers, in good agreement with the estimate proposed by Kogan of 1-10 V for ionic solids[1], and comparable to the value found for other perovskites such as lead magnesium niobate-lead titanate (PMN-PT)[23]. The similarity of the coefficients measured by inverse and direct methods also provides experimental validation that flexoelectric devices will display the same coupling constant for operation as sensor and actuator[13].

We now turn to the comparison between the actuation performance of the flexoelectric cantilevers and that of state of the art piezoelectric bimorph cantilevers fabricated using Zinc oxide (ZnO)[24], Aluminium nitride (AlN)[25], PZT[22], and PMN-PT[26]. This is shown in **Figure 4**. The electromechanical performance, or the curvature/electric field ratio, of our $SrTiO_3$ devices (3.33 MV^{-1}) is comparable to or larger than that of devices fabricated using ZnO[24] (0.044 MV^{-1}), and AlN[25] (0.133 MV^{-1}) and PZT[22] (5.208 MV^{-1}). The performance of our flexoelectric devices is, however, lower than that of hyper-active PMN-PT[26] (184.4 MV^{-1}) and an optimal ultra-thin device made with a 10 nm thick AlN[27] (50.3 MV^{-1}) active layer. However, the *flexoelectric curvature/voltage* scales as the inverse of the cube of the thickness (eq. 1), so $SrTiO_3$ devices with the same thickness as the state of the art AlN[27] could exceed the performance of even the best piezoelectric and ferroelectric devices so far reported in literature. We have also programmed an open access App (https://umeshkbhaskar.shinyapps.io/FlexovsPiezo_app) to facilitate direct comparison between the expected performance of piezoelectric and flexoelectric actuators for different cantilever geometries and material specifications.

In conclusion, we have shown that flexoelectricity can be exploited to fabricate lead-free electromechanical actuators which can be integrated on silicon for MEMS and NEMS applications. Looking beyond $SrTiO_3$, all high-k dielectric materials used in CMOS circuitry should in principle also be flexoelectric, because this is a property that is not restricted by material symmetry[9]. Therefore, an extensive catalogue of materials is likely to be suitable for nanoscale electromechanical device applications providing a route to integrating “more than Moore” electromechanical functionalities within transistor technology.

FIGURES

Figure 1 Schematic illustration of flexoelectric actuation versus piezoelectric bimorph actuation in nanoscale actuators. In a piezoelectric bimorph actuator, a homogenous mechanical strain is generated on application of an electrical voltage to the piezoelectric layer; the mechanical clamping induced by the non-piezoelectric layer creates a strain gradient across the structure, converting the piezoelectric strain in to a flexural motion. On the other hand, any dielectric sandwiched between electrodes can in principle act as a flexoelectric actuator. In this case, the bending moment arises from a symmetry breaking strain gradient generated at the unit cell level

Figure 2 Experimental design (a) Optical image of an array of $SrTiO_3$ nanocantilevers; (b) 3D image of one $SrTiO_3$ nanocantilever with colour scale corresponding to the out of plane displacement; (c) The digital holographic microscope splits a coherent laser beam in to an objective beam and a reference beam. The objective beam is focused on the sample, and the light reflected is collected to form an interference pattern with the reference beam. Any difference in height along the sample surface results in a corresponding difference in phase of the light reflected back from it.

Figure 3 Experimental characterisation of flexoelectricity as a function of frequency and electric field. The AC voltage, and first harmonic displacement, for an applied voltage of 1 V plotted for the cantilever (a) below and (b) above the resonance frequency. (c) The Curvature/Voltage ratio as a function of the frequency for the $SrTiO_3$ nanocantilever at 1V excitation, showing the resonant peak at ~310 KHz. The quality factor Q is ~ 25. The resonance is confirmed by the 180^o phase change. (d) The first harmonic flexoelectric curvature shows a linear variance when plotted as a function of the applied AC field. The frequency of the measurement was 100 KHz,

well below the resonant frequency amplification and close to the static performance calculated from the fit in (c).

Figure 4 Comparison of the performance of flexoelectric $SrTiO_3$ with that of the state of the art piezoelectric bimorphs. The ratio of Curvature/Electric field is compared for a flexoelectric $SrTiO_3$, and piezoelectric devices fabricated from ZnO[24], AlN[25,27], PZT[22], and PMN-PT[26]. For all materials, we quote the intrinsic response measured out of resonance.

ACKNOWLEDGMENT

The work at ICN2 was funded by an ERC Starting Grant from the EU (Project No. 308023), a National Plan grant from Spain (FIS2013-48668-C2-1-P) and the Severo Ochoa Excellence programme. The work at Cornell University was supported by the National Science Foundation (Nanosystems Engineering Research Center for Translational Applications of Nanoscale Multiferroic Systems) under grant number EEC-1160504. The authors are grateful to discussions with Etienne Cuche, Jerome Parent, Eduardo Solanas and Yves Emery.

Author Contributions

[+]Both authors contributed equally.

G.C and U.B conceived and designed the experiments; N.B designed and made the cantilevers under the supervision of G.R; U.B performed and analysed the inverse flexoelectric characterizations under the supervision of G.C; A.A performed the self-consistent continuum modelling and simulations; Z.W performed the Molecular beam epitaxy growth of the template layer under the supervision of D.S; U.B. and G. C. wrote the paper with the help of all other authors. All authors discussed the results, commented on the manuscript and have given their approval to the final version of the manuscript.

Additional information

Supplementary information accompanies this paper at www.nature.com/naturenanotechnology.

Reprints and permission information is available online at

http://npg.nature.com/reprintsandpermissions/.

Correspondence and requests for materials should be addressed to U.B and G.C.

REFERENCES

1. Kogan, S. Piezoelectric effect during inhomogeneous deformation and acoustic scattering of carriers in crystals. *Sov. Phys. Solid State* **5,** 2069–2079 (1964).

2. Bursian, E. & Trunov, N. Nonlocal piezoelectric effect. *Sov. Phys. Solid State* **16,** 760–762 (1974).

3. Gregg, J. M. Stressing Ferroelectrics. *Science* **336,** 41–42 (2012).

4. Majdoub, M., Sharma, P. & Çağin, T. Dramatic enhancement in energy harvesting for a narrow range of dimensions in piezoelectric nanostructures. *Phys. Rev. B* **78,** 121407 (2008).

5. Lee, D. *et al.* Giant flexoelectric effect in ferroelectric epitaxial thin films. *Phys. Rev. Lett.* **107,** 057602 (2011).

6. Cross, L. Flexoelectric effects: Charge separation in insulating solids subjected to elastic strain gradients. *J. Mater. Sci.* **41,** 53–63 (2006).

7. Cross, E. Lead-free at last. *Nature* **32,** 24–25 (2004).

8. Dreyfus, R. *et al.* Microscopic artificial swimmers. *Nature* **437,** 862–865 (2005).

9. Zubko, P., Catalan, G. & Tagantsev, A. K. Flexoelectric Effect in Solids. *Annu. Rev. Mater. Res.* **43,** 387–421 (2013).

10. Biancoli, A., Fancher, C. M., Jones, J. L. & Damjanovic, D. Breaking of macroscopic centric symmetry in paraelectric phases of ferroelectric materials and implications for flexoelectricity. *Nat. Mater.* **14,** 224–229 (2014).

11. Cross, L. Flexoelectric effects: Charge separation in insulating solids subjected to elastic strain gradients. *J. Mater. Sci.* **41,** 53–63 (2006).

12. Zubko, P., Catalan, G., Buckley, A., Welche, P. & Scott, J. Strain-Gradient-Induced Polarization in $SrTiO_3$ Single Crystals. *Phys. Rev. Lett.* **99,** 167601 (2007).

13. Breger, L., Furukawa, T. & Fukada, E. Bending piezoelectricity in polyvinylidene fluoride. *Jpn. J. Appl. Phys.* **15,** 2239–40 (1976).

14. Tagantsev, A. K. & Yurkov, A. S. Flexoelectric effect in finite samples. *J. Appl. Phys.* **112,** 044103 (2012).

15. Bursian, E. & Zaikovskii, O. I. Changes in curvature of ferroelectric film due to polarization. *Sov. Phys. Solid State* **10,** 1121 (1968).

16. Abdollahi, A., Peco, C., Millán, D., Arroyo, M., & Arias, I.. Computational evaluation of the flexoelectric effect in dielectric solids. *J. Appl. Phys* **116**, 093502 (2014).

17. Zalesskii, V. G. & Rumyantseva, E. D. Converse flexoelectric effect in the SrTiO3 single crystal. *Phys. Solid State* **56,** 1352–1354 (2014).

18. Deng, Q., Liu, L. & Sharma, P. Electrets in soft materials: Nonlinearity, size effects, and giant electromechanical coupling. *Phys. Rev. E, Soft Matter Phys.* **90,** 1–7 (2014).

19. Baek, S.-H. & Eom, C.-B. Epitaxial integration of perovskite-based multifunctional oxides on silicon. *Acta Mater.* **61,** 2734–2750 (2013).

20. Cotte, Y., Toy, F., Jourdain, P. & Pavillon, N. Marker-free phase nanoscopy. *Nat. Photonics* **7,** 113–117 (2013).

21. Colomb, T., Krivec, S. & Hutter, H. Digital holographic reflectometry. *Opt. Express* **21,** 12643–12650 (2013).

22. Dekkers, M. *et al.* The significance of the piezoelectric coefficient d_{31}eff determined from cantilever structures. *J. Micromechanics Microengineering* **23,** 025008 (2013).

23. Narvaez, J. & Catalan, G. Origin of the enhanced flexoelectricity of relaxor ferroelectrics. *Appl. Phys. Lett.* **104,** 162903 (2014).

24. Wang, P., Du, H., Shen, S., Zhang, M. & Liu, B. Preparation and characterization of ZnO microcantilever for nanoactuation. *Nanoscale Res. Lett.* **7,** 176 (2012).

25. Doll, J. C., Petzold, B. C., Ninan, B., Mullapudi, R. & Pruitt, B. L. Aluminum nitride on titanium for CMOS compatible piezoelectric transducers. *Journal of Micromechanics and Microengineering* **20,** 025008 (2009).

26. Baek, S. H. *et al.* Giant Piezoelectricity on Si for Hyperactive MEMS. *Science* **334,** 958–961 (2011).

27. Zaghloul, U. & Piazza, G. 10-25 NM piezoelectric nano-actuators and NEMS switches for millivolt computational logic. *Proc. IEEE Int. Conf. Micro Electro Mech. Syst.* 233–236 (2013). doi:10.1109/MEMSYS.2013.6474220

Methods

Fabrication of nanocantilevers

All-oxide epitaxial flexoelectric MEMS devices were grown using pulsed laser deposition patterned using a lift-off[28] method, and finally released via anisotropic substrate etching (as shown in Supplementary Figure 1). To ensure the (00l) epitaxial growth of the perovskites on Si, an epitaxial $SrTiO_3$ buffer layer (~ 30 nm) was grown by molecular beam epitaxy (MBE)[29]. The functional $SrTiO_3$ layer (~ 70 nm), embedded between the $SrRuO_3$ (~ 25 nm) electrode layers were grown epitaxially (Supplementary Figure 2) using pulsed laser deposition. A sacrificial mask assisted lift-off technique was utilized to pattern the heterostructures, in a single lift-off step[28]. The top $SrRuO_3$ electrode layer was patterned using ion-beam etching. After patterning the perovskite layers, the free-standing devices were released by anisotropic KOH etching of the Si substrate. Owing to the difference in number of exposed dangling bonds for different crystal planes of Si, a strong anisotropy exists in the etching rate. Hence, control of the cantilever in-plane orientation with respect to the substrate crystal axis is crucial for achieving the desired release rate and minimizing any etching related damages[30] . The released length of the cantilever plate is 16 um.

Detection of cantilever vibrations using the DHM

The DHM synchronizes the image acquisition frequency with the frequency of sinusoidal excitation applied to the cantilever to ensure that the periodic movement of the cantilever is completely captured as a sequential array of static holograms. Each hologram captured by the DHM (**Figure 1c**) is simultaneously resolved in to an intensity image, which is similar to a single wavelength microscope image, and a phase image, which maps the topographic profile of

the sample. The phase images calculate the topography based on the path difference of light reflected by the surface compared to a specified reference frame; by placing this reference on the base of the cantilever, each phase image provides us with the full profile –including the curvature– of the cantilever. By its nature, the measurement is insensitive to any voltage induced homogenous expansions or deformations, and only records voltage induced changes in the slope and curvature of the cantilever. The periodic displacement in response to an applied AC excitation was found to contain both first harmonic (1ω) and second harmonic contributions (2ω). In order to get the strength of purely the flexoelectric response (which is linearly proportional to the field and therefore a first harmonic oscillation) Fourier filtering or harmonic regression was employed to quantify the 1ω bending.

Self-consistent continuum model of flexoelectricity

By employing a self-consistent continuum model of flexoelectricity[16], we perform simulations of the multilayer cantilever beam under the application of an electric field. The aspect ratio of the beam is fixed to $L/h = 10$, where L and h are the length and height of the beam. A larger aspect ratio leads to almost identical results. The electrical potential is fixed to zero on the top electrode and we constrain the electric potential on the bottom electrode to a constant value, generating the same magnitude of the applied electric field as in experiments. The material parameters are chosen according to the composition of the multilayer cantilever. Given that there is not yet a universal consensus regarding the size, or even the sign, of the flexoelectric coefficients for any material, we consider $\mu_{12} = -10\mu_{11}$, a limiting case reported from the direct measurement on STO[12]. Simulation results show that the cantilever is deflected under the applied electrical load,

supporting the experimental observations that a cantilever beam can deform as an electromechanical actuator due to flexoelectricity.

28. Banerjee, N., Koster, G. & Rijnders, G. Submicron patterning of epitaxial $PbZr_{0.52}Ti_{0.48}O_3$ heterostructures. *Appl. Phys. Lett.* **102**, 142909 (2013).

29. Warusawithana, M. P. *et al.* A ferroelectric oxide made directly on silicon. *Science* **324,** 367–370 (2009).

30. Banerjee, N., Houwman, E. P., Koster, G. & Rijnders, G. Fabrication of piezodriven, free-standing, all-oxide heteroepitaxial cantilevers on silicon. *Apl Mater*. **2,** 096103 (2014)

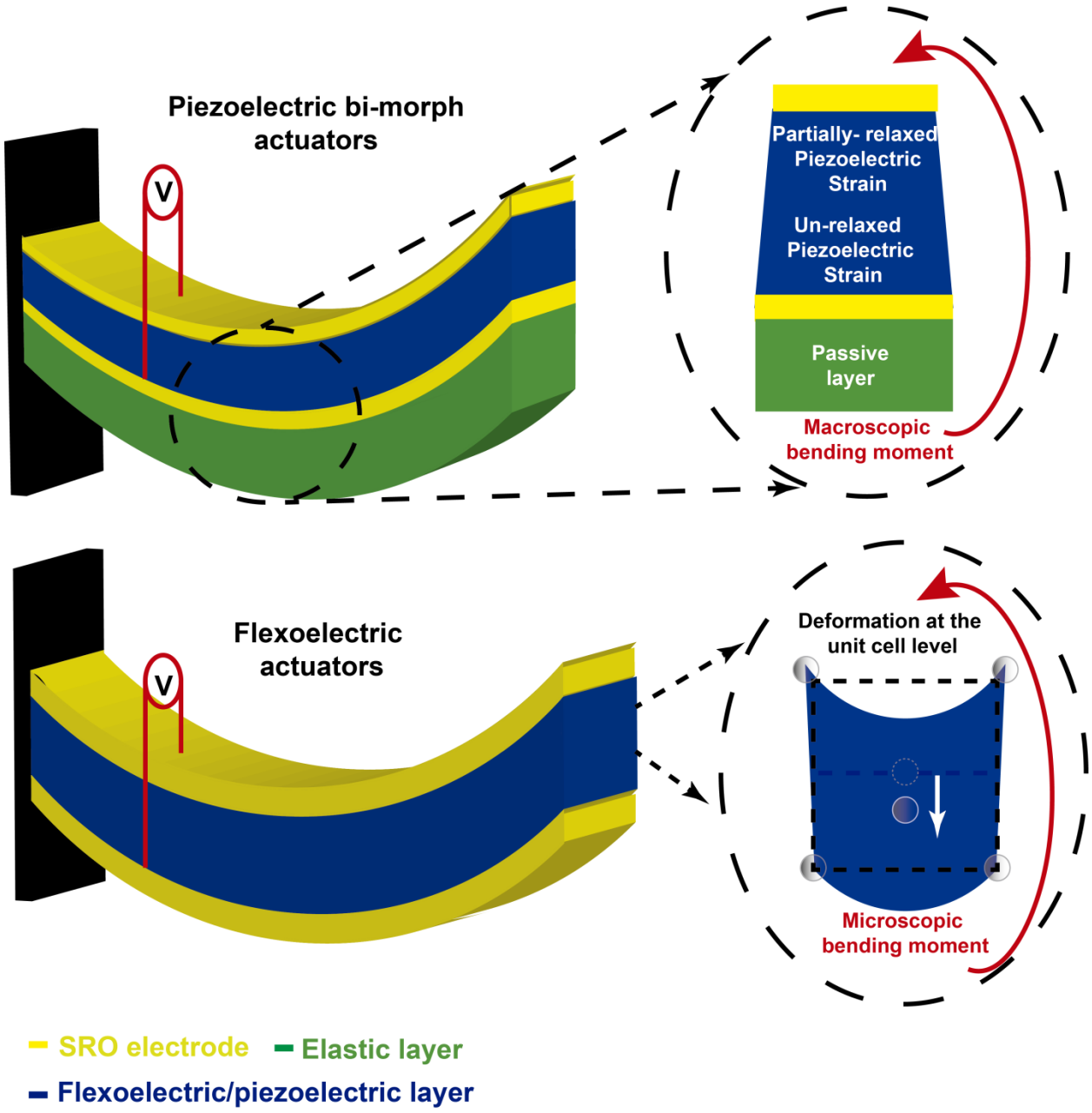
Piezoelectric bi-morph actuators
V
Partially- relaxed Piezoelectric Strain
Un-relaxed Piezoelectric Strain
Passive layer
Macroscopic bending moment
Flexoelectric actuators
V
Deformation at the unit cell level
Microscopic bending moment
SRO electrode
Elastic layer
Flexoelectric/piezoelectric layer

Figure 1

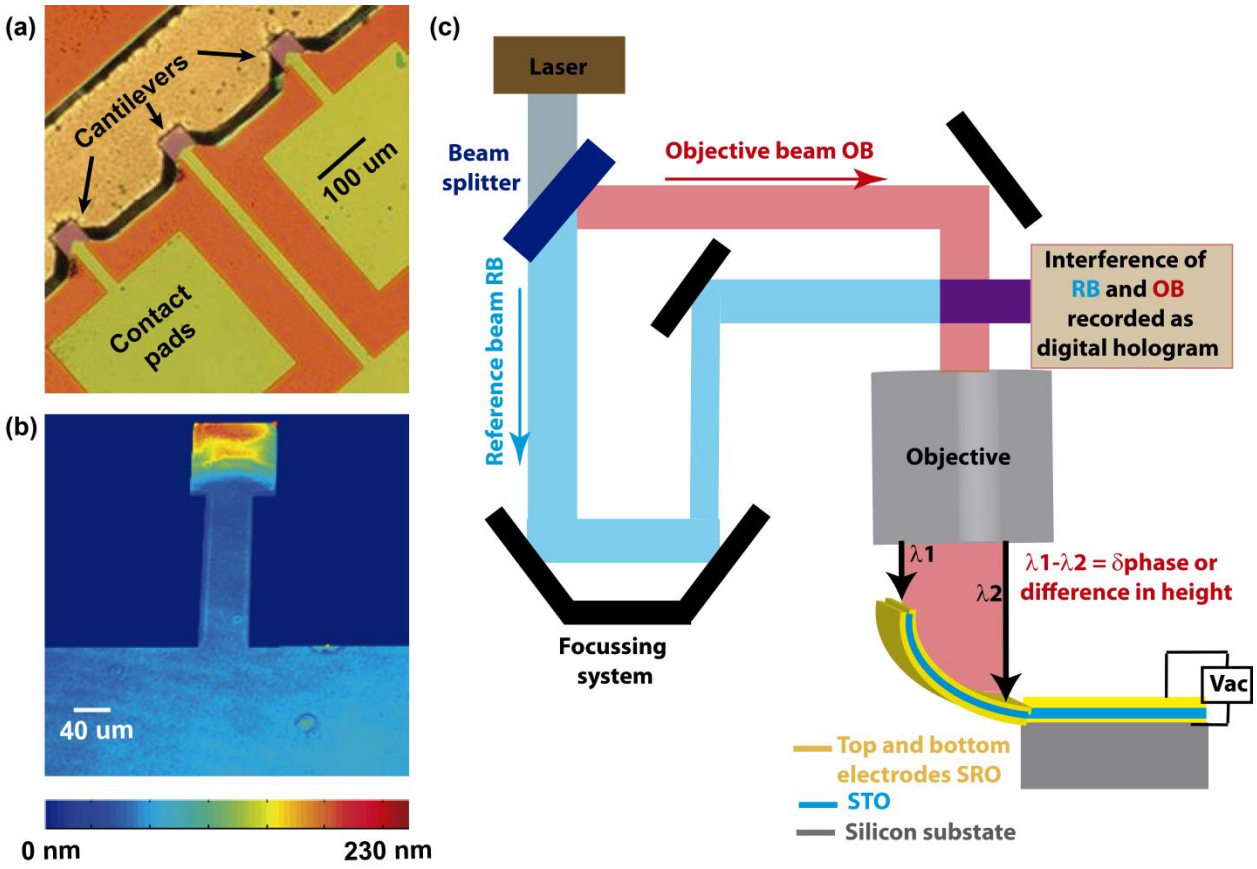
(a)
Cantilevers
100 um
Contact pads
(b)
40 um
0 nm
230 nm
(c)
Laser
Beam splitter
Objective beam OB
Reference beam RB
Interference of RB and OB recorded as digital hologram
Objective
λ1
λ2
λ1-λ2 = δphase or difference in height
Focussing system
Vac
Top and bottom electrodes SRO
STO
Silicon substate

Figure 2

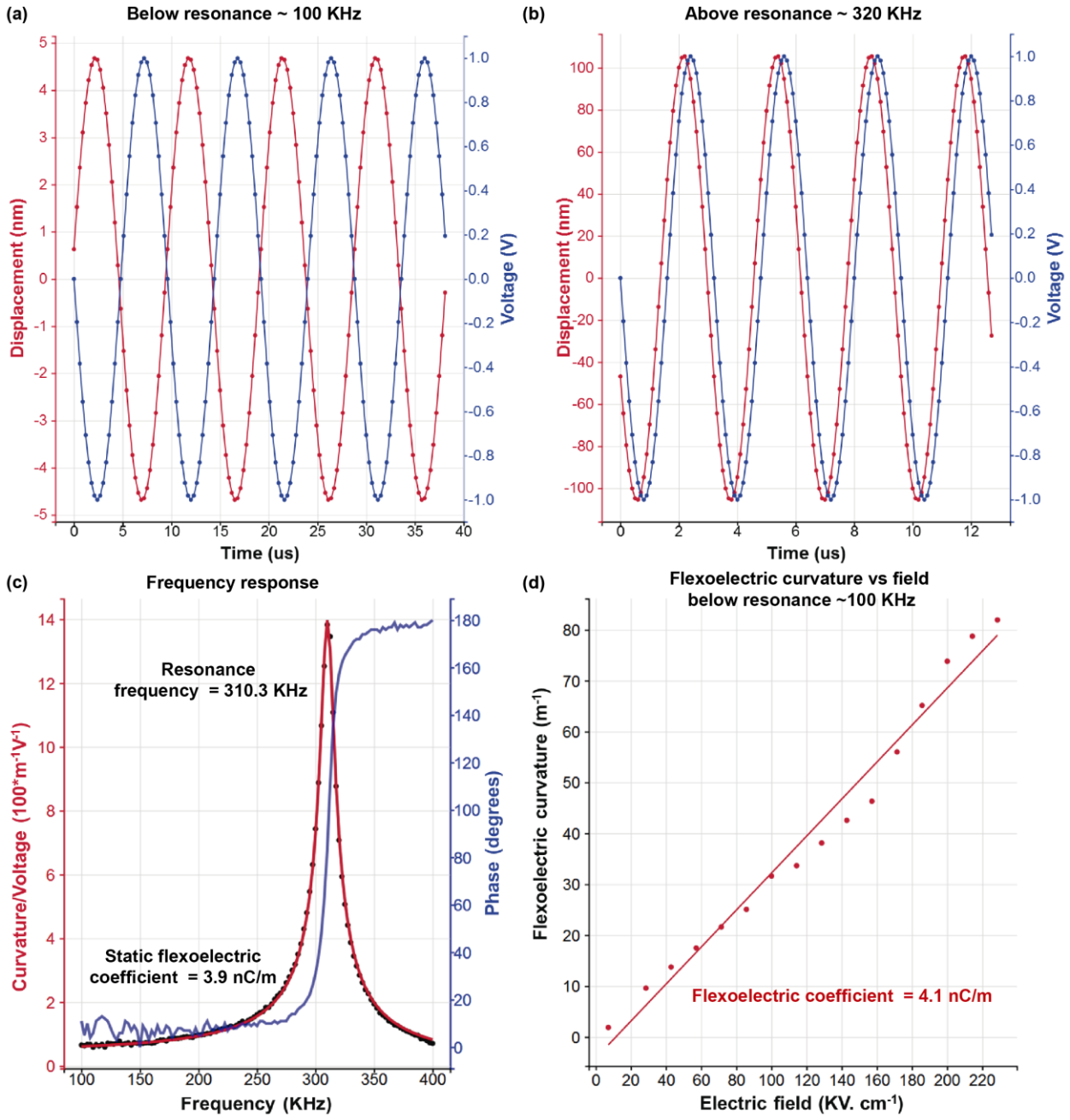
(a)
Below resonance ~ 100 KHz
Displacement (nm)
Voltage (V)
Time (us)
(b)
Above resonance ~ 320 KHz
Displacement (nm)
Voltage (V)
Time (us)
(c)
Frequency response
Resonance
frequency = 310.3 KHz
Static flexoelectric
coefficient = 3.9 nC/m
Curvature/Voltage (100*m-1V-1)
Phase (degrees)
Frequency (KHz)
(d)
Flexoelectric curvature vs field
below resonance ~100 KHz
Flexoelectric curvature (m-1)
Flexoelectric coefficient = 4.1 nC/m
Electric field (KV. cm-1)

Figure 3

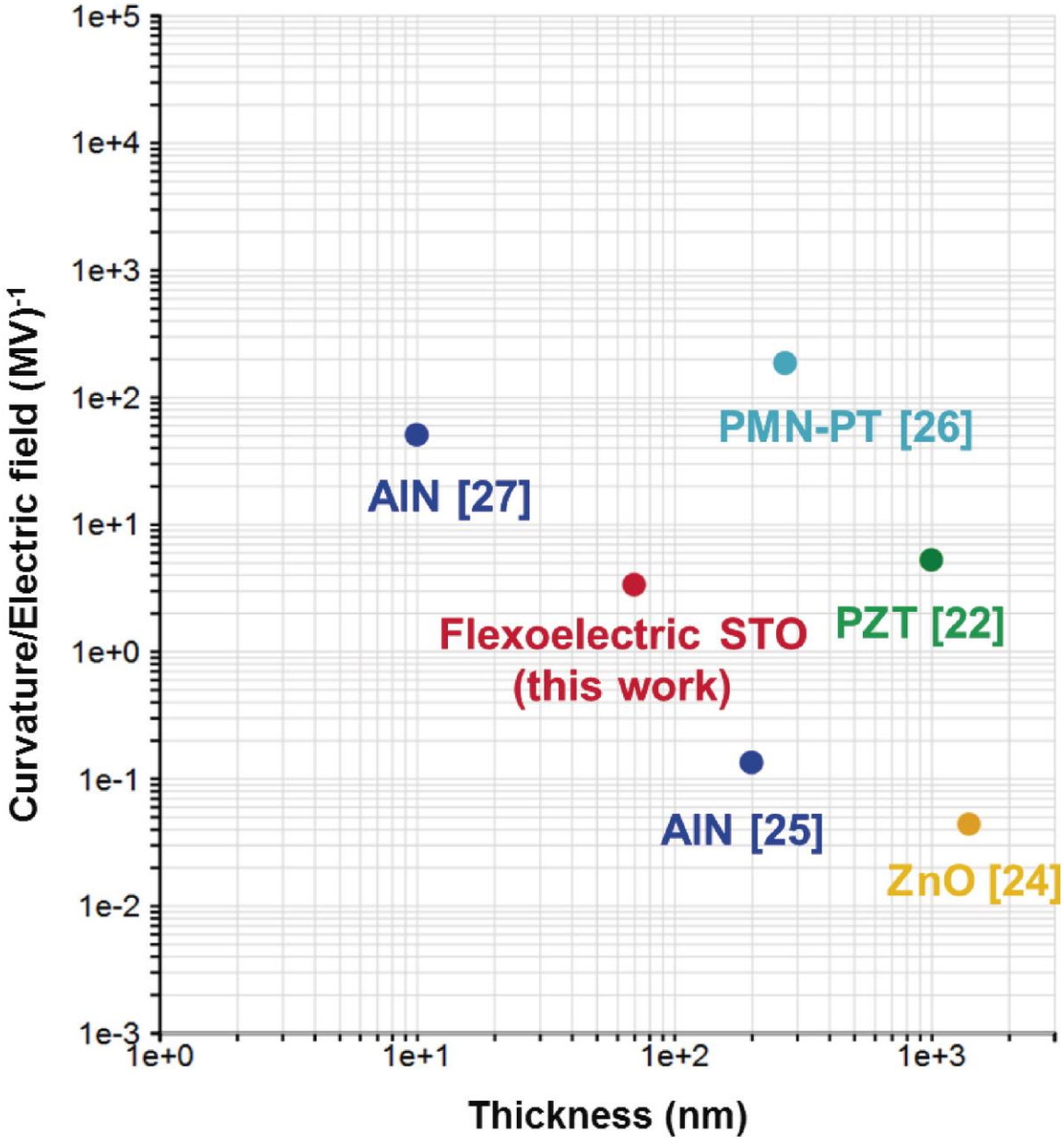
Curvature/Electric field (MV)-1
1e+5
1e+4
1e+3
1e+2
1e+1
1e+0
1e-1
1e-2
1e-3
1e+0
1e+1
1e+2
1e+3
Thickness (nm)
PMN-PT [26]
AlN [27]
PZT [22]
Flexoelectric STO
(this work)
AlN [25]
ZnO [24]

Figure 4